

Computer simulations of the Gardner transition in structural glasses

Yuliang Jin^{1,2,3} and Hajime Yoshino^{4,5}

¹*CAS Key Laboratory of Theoretical Physics, Institute of Theoretical Physics,
Chinese Academy of Sciences, Beijing 100190, China*

²*School of Physical Sciences, University of Chinese Academy of Sciences, Beijing 100049, China*

³*Wenzhou Institute, University of Chinese Academy of Sciences, Wenzhou, Zhejiang 325000, China*

⁴*Cybermedia Center, Osaka University, Toyonaka, Osaka 560-0043, Japan*

⁵*Graduate School of Science, Osaka University, Toyonaka, Osaka 560-0043, Japan*

CONTENTS

I. Connections between Gardner and spin-glass transitions	1
II. Gardner transition under compression	3
A. Preparation of ultra-stable glasses	3
B. Key observables and protocols	4
C. Aging effects	5
D. Anomalous order parameters and responses	5
III. Gardner transition under shear	6
IV. Discussion and outlook	6
References	7

I. CONNECTIONS BETWEEN GARDNER AND SPIN-GLASS TRANSITIONS

The exact mean-field theory for the simplest glass-forming system - the dense assembly of hard spheres in the large dimensional limit - predicts the existence of a Gardner phase [1, 2]. This transition is characterized by full replica symmetry breaking (RSB) that implies two fascinating physical consequences. (i) A hierarchical free-energy landscape, i.e., the thermal fluctuations are organized hierarchically, meaning that configurations are grouped into meta-basins that are further grouped into meta-meta basins, ... (ii) The marginal stability, i.e., the system responds sensitively to infinitesimal perturbations. Here we discuss recent results of numerical simulations to examine these mean-field predictions in physical dimensions.

From the viewpoint of RSB, the Gardner transition in structural glasses belongs to the same full RSB universality class of the spin-glass transition (see Fig. 1(A)). This theoretical ground motivates us to borrow ideas from the extensive research on spin-glasses to study the Gardner transition. To this end, it is useful to review firstly some of the essential results obtained in spin-glass experiments and simulations.

The RSB solution immediately implies a hierarchy of linear responses through the fluctuation-dissipation relation [3]. One expects short-time, intermediate-time, and long-time linear responses associated with thermal fluctuations inside basins, meta-basins, and meta-meta-basins. A remarkable consequence is the “anomaly” that gives a natural explanation for the protocol-dependent linear responses observed experimentally [4]. In one protocol called *field cooling* (FC), one measures the magnetization m_{FC} of a spin-glass under cooling from a high temperature T_{max} down to a low temperature T_{min} below the spin-glass transition temperature T_{SG} in the presence of a weak external magnetic field δh ; in the other protocol called *zero field cooling* (ZFC), one cools the spin-glass from T_{max} down to T_{min} without the field ($h = 0$), then switches on the magnetic field δh and measures the magnetization m_{ZFC} under heating the spin-glass back to T_{max} (see Fig. 1(B)). The two susceptibilities $\chi_{\text{FC}} = m_{\text{FC}}/\delta h$ and $\chi_{\text{ZFC}} = m_{\text{ZFC}}/\delta h$ are the same above T_{SG} , but different ($\chi_{\text{FC}} > \chi_{\text{ZFC}}$) below (see Fig. 2(A)). The fact that χ_{FC} and χ_{ZFC} are different in the spin-glass phase is referred to as an “anomaly”, because the susceptibility is protocol-independent in standard magnetic systems. The RSB theory gives $\chi_{\text{FC}} - \chi_{\text{ZFC}} = \beta \left[\int_0^1 dq P(q)q - q_{\text{EA}} \right]$, with β the inverse temperature. Here q_{EA} is the Edwards-Anderson (EA) order parameter [5] representing the strength of the thermal fluctuation within lowest-level basins, while $\int_0^1 dq P(q)q$ represents the integral of thermal fluctuations coming from all levels in the hierarchy. In the replica symmetric (RS) solution, $P(q) = \delta(q - q_{\text{EA}})$, so that the anomaly vanishes.

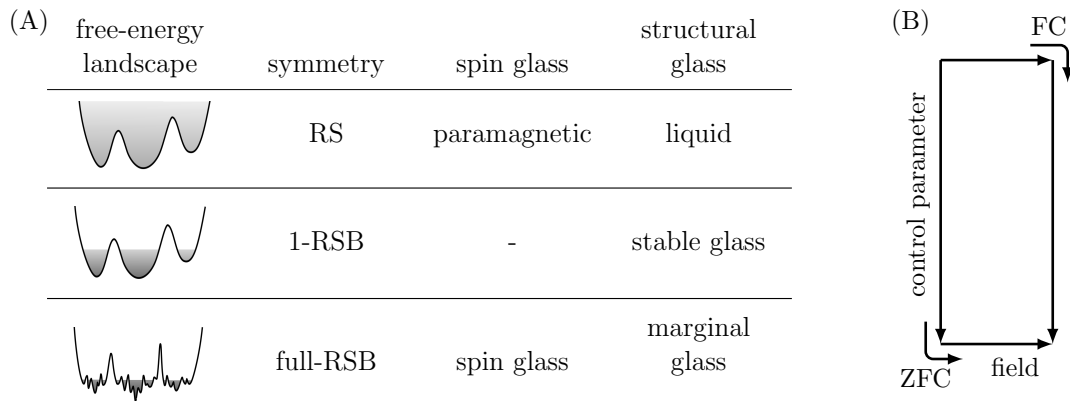


FIG. 1. (A) Correspondence between spin and structural glasses. Note that one step RSB (1-RSB) exists in certain spin-glass models such as the spherical p -spin ($p > 2$) model [6]. (B) Schematic of ZFC/FC protocols. In spin and hard-sphere glasses, the control parameter is the temperature T and the density (volume fraction) φ respectively, and the external field is the magnetic field h and the shear-strain γ respectively.

The anomaly is known to be not a transient but a long-time effect, as demonstrated by a series of experiments that reveal aging effects in spin-glasses [7–9]. To study the dynamical effects, one can generalize the ZFC protocol by introducing a waiting time t_w before switching on the magnetic field, and a measurement time τ elapsed in the presence of the field. By increasing τ , $m_{\text{ZFC}}(\tau, t_w)$ increases passing through m_{ZFC} and heads toward m_{FC} (see Fig. 2(B)). However, $m_{\text{ZFC}}(\tau, t_w)$ does not reach m_{FC} within finite time, and its time evolution as a function of τ slows down with increasing waiting time t_w , manifested by scaling laws depending on τ/t_w . These experimental observations are significant because they reveal the out-of-equilibrium nature of spin-glasses. To describe the aging effects and the anomaly from a purely dynamical point of view, a dynamical mean-field theory on spin-glass models is developed [10, 11]. The dynamical theory relates RSB to the notion of effective temperature that characterizes out-of-equilibrium glassy dynamics [12, 13]. The numerical evidence of effective temperature [14] and non-zero anomaly in the long-time limit [15] has been indicated by detailed simulations of finite-dimensional spin-glass models.

The marginal stability of the spin-glass phase may account for various complex non-linear responses, such as the effect of static chaos with respect to an infinitesimal change of temperature, or avalanches with respect to an infinitesimal change of magnetic field. Indeed the equilibrium spin configurations at large length scales are completely reshuffled by infinitesimal perturbations, which is predicted first by the droplet theory [16–18], and later by theories based on RSB [19–26]. The rejuvenation-memory effects observed experimentally [27] may be related to such non-linear responses [28, 29].

Once one is aware of the correspondence between spin and structural glasses (see Fig. 1(A)), it is natural to use strategies inherited from spin-glass studies to explore the physics of Gardner phase in structural glasses. For example, in the ZFC/FC protocols, the role of the magnetic field h for spin-glasses can be replaced by the shear strain γ for structural glasses (see Fig. 1(B)), which only changes the boundary condition but not the thermodynamic properties of the bulk. Indeed, the replica theory of structural glasses predicts a hierarchy of shear moduli reflecting RSB [30–32]. By adapting the methods developed in spin-glasses, one can examine the aging effects, the protocol-dependent linear responses, and the non-linear responses such as avalanches, in structural glasses with respect to shear deformations. Our discussion focuses on one of the simplest models of structural glasses in three dimensions, hard spheres, where the (reduced) pressure p (or the volume fraction φ) plays the role of temperature T . According to the replica theory [1] that is exact in the large dimensional limit, a Gardner transition occurs in hard spheres under both compression and shear, which is examined by simulations at three-dimensions in the following sections. The dynamical mean-field theory for the hard-sphere glass has also been set up [33–36], but a detailed theoretical analysis of the out-of-equilibrium dynamics remains challenging. Nonetheless, the analogy to the spin-glass problem outlined above allows us to infer the implications of RSB on the dynamics of hard spheres.

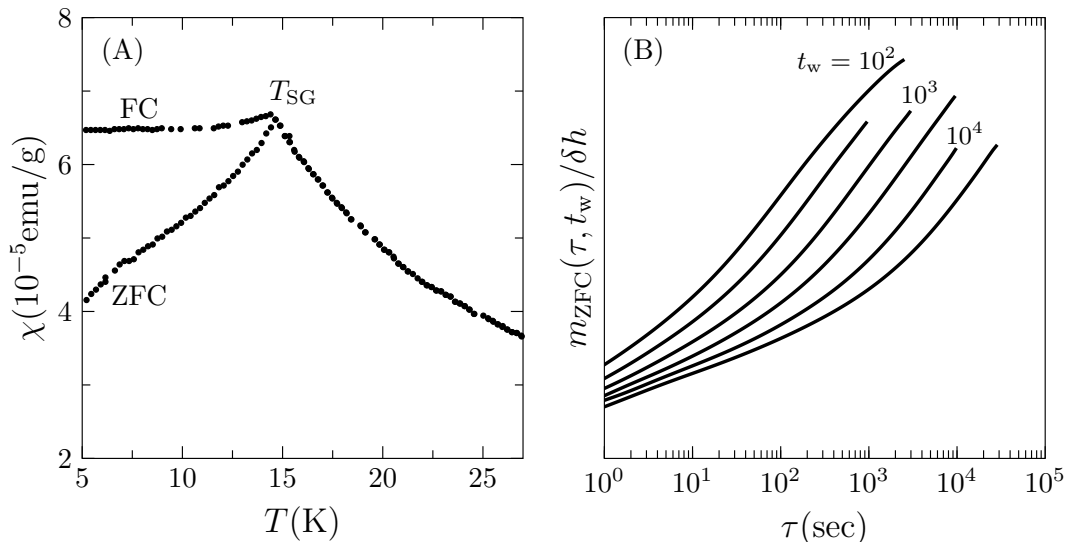


FIG. 2. Experimental results on CuMn spin-glasses. (A) ZFC/FC susceptibilities (adapted from [4]), and (B) the time evolution of $m_{ZFC}(\tau, t_w)/\delta h$ in an aging experiment (adapted from [7]).

II. GARDNER TRANSITION UNDER COMPRESSION

A. Preparation of ultra-stable glasses

To study the Gardner transition, we must prepare a glass at first. Experimentally, glasses are obtained by a slow thermal or compression annealing, the rate of which determines the location of the glass transition. It is found that a detailed numerical analysis of the Gardner transition requires the preparation of extremely well-relaxed glasses (corresponding to structural relaxation timescales challenging to simulate in standard algorithms), in order to study vibrational motions of particles without interference from diffusion. Such ultra-stable glasses can be numerically generated by applying a swap Monte-Carlo scheme [37, 38] to a simple glass-forming model – a polydisperse mixture of N hard spheres [39].

The annealing procedure contains two steps [39]. First, one produces equilibrated liquid configurations at various densities φ_g with the help of the swap algorithm. Second, starting from these liquid configurations, one switches to standard molecular dynamics simulations [40] during which the system is compressed out of equilibrium up to target densities $\varphi > \varphi_g$. In order to obtain thermal and disorder averaging, this procedure is repeated over many samples, each corresponding to different initial equilibrium configurations at φ_g , and over many independent quench realizations for each sample. The independent realizations of the same sample have identical particle positions at φ_g , but are assigned to different initial velocities drawn from the Maxwell–Boltzmann distribution.

The above numerical protocol is analogous to thermal annealing with different cooling rates, which results in different glass transition temperatures. Each glass transition density φ_g selects a particular glass state. The value of φ_g ranges from the mode-coupling theory (MCT) density (or the dynamical glass transition density) φ_d , at which the liquid relaxation is slow but affected by activated α -processes, to $\varphi_g \gg \varphi_d$, where particle diffusion and vibrations are fully separated. For sufficiently large φ_g , the α -relaxation time becomes larger than the simulation time by many orders of magnitude; one thus obtains unimpeded access to the dynamics within the glass state, i.e., the β -relaxation processes [41].

The liquid equation of state (EOS) for the reduced pressure $p = \beta P/\rho$ of the model, where ρ is the number density, and P the system pressure, can be well described by the Carnahan–Starling (CS) equation [42]. The dynamical glass transition density $\varphi_d = 0.594(1)$ was estimated following the strategy in Ref. [43]. Note that the dynamical glass transition is only rigorous in large dimensions; it becomes a dynamical crossover in three dimensions (see Chapter 16 for a detailed discussion). The non-equilibrium glass EOSs associated with compression terminate at inherent states (where $p \rightarrow \infty$) that correspond to, for hard spheres, jammed configurations at φ_J , and can be captured by a free-volume scaling form, $p_{\text{glass}}(\varphi) \sim (\varphi_J - \varphi)$ [44]. Figure 3 presents the phase diagram and EOSs of the model.

Along each glass EOS of a given φ_g , a corresponding Gardner transition may exist at density φ_G (or pressure p_G), as predicted by the mean-field theory. For $\varphi_g < \varphi < \varphi_G$, the system is in a *stable glass* phase: each glass state is confined in one of the structureless basins on the free-energy landscape (see Fig. 1(A)), and is stable in response to

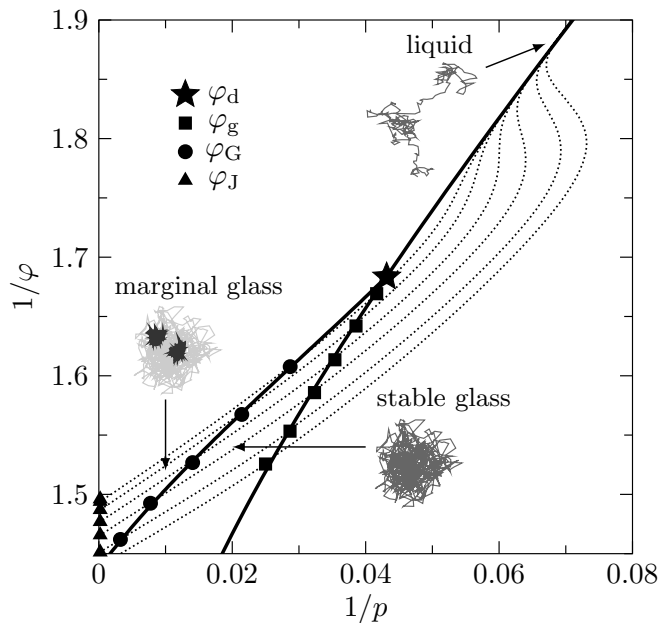


FIG. 3. Phase diagram of a polydisperse hard-sphere glass in three dimensions (adapted from [39]). Solids lines represent the CS liquid EOS and the Gardner line, and dashed lines represent glass EOSs. The insets show typical particle motions in three phases.

small mechanical deformations. On the other hand, the regime $\varphi_G < \varphi < \varphi_J$ corresponds to a *marginal glass* phase, where each simple glass basin splits into a fractal hierarchy of sub-basins and the glass becomes marginally stable to deformations. The Gardner line and the liquid EOS merge around φ_d , suggesting the mixing of dynamical behavior associated to the Gardner transition and to the glass transition – this is why one needs to focus on ultra-stable glasses in order to explore pure Gardner physics.

B. Key observables and protocols

In the glass state, particles vibrate inside their cages (see the insets of Fig. 3). The first approach to study the Gardner transition is based on the direct analysis of *caging order parameters*, which quantify the caging properties of particles. In the case of stable glasses, the caging order parameter is defined as, $\Delta_{EA} = \lim_{t \rightarrow \infty} \frac{1}{N} \sum_{i=1}^N \langle |\vec{r}_i(t) - \vec{r}_i(0)|^2 \rangle$, where $\vec{r}_i(t)$ is the position of particle i at time t . The parameter Δ_{EA} , which decreases with the degree of annealing, corresponds to nothing but the EA parameter q_{EA} in spin-glasses.

Similar to the spin-glass transition, the Gardner transition induces the split of basins on the free-energy landscape and aging effects, which suggests that the order parameter must be generalized: one considers (i) the mean-squared displacement (MSD) $\Delta(\tau, t_w)$ and (ii) the distance between pairs of independently quenched configurations $\Delta_{AB}(t)$. Here the MSD is defined as, $\Delta(\tau, t_w) = \frac{1}{N} \sum_{i=1}^N \langle |\vec{r}_i(\tau + t_w) - \vec{r}_i(t_w)|^2 \rangle$, averaged over both thermal fluctuations and disorder, at the target φ reached by compression. A waiting time t_w is introduced in order to explicitly examine the aging effects (the total time t is the sum of the measurement time τ and t_w). On the other hand, $\Delta_{AB}(t) = \frac{1}{N} \sum_{i=1}^N \langle |\vec{r}_i^A(t) - \vec{r}_i^B(t)|^2 \rangle$, where the two copies A and B are independent realizations at φ , compressed from the same initial sample at φ_g .

The large-time limits of these quantities have important physical meanings. The EA order parameter is defined as $\Delta_{EA} \equiv \lim_{\tau \rightarrow \infty} \lim_{t_w \rightarrow \infty} \Delta(\tau, t_w)$. Here the order of time limits is crucial [45]: by reversing the order one can define another parameter, $\Delta_{AB} \equiv \lim_{t_w \rightarrow \infty} \lim_{\tau \rightarrow \infty} \Delta(\tau, t_w) = \lim_{t \rightarrow \infty} \Delta_{AB}(t)$. The RSB is signaled by $\Delta_{AB} > \Delta_{EA}$ (note that $\Delta_{AB} = \Delta_{EA}$ in stable glasses). In other words, the two large-time limits cannot be interchanged in the Gardner phase, meaning that the aging effects become persistent.

In the second approach, one studies the response of hard-sphere glasses against a shear strain γ , analogous to observing magnetic susceptibilities in spin-glasses. The simple strain γ is applied to the x -coordinates of all particles ($x_i \rightarrow x_i + \gamma z_i$) after a waiting time t_w , under the constant-volume and Lees-Edwards boundary conditions [46]. The strain is increased slowly with a constant shear rate $\dot{\gamma}$, and the reduced shear stress $\sigma = \beta \Sigma / \rho$ is measured, where Σ

is the stress (for convenience, some data are presented with the unitless stress rescaled by pressure, $\tilde{\sigma} = \sigma/p$).

As in the spin-glass case, one can consider two types of protocols, namely *zero field compression* (ZFC) and *field compression* (FC) (see Fig. 1 (B)). In the ZFC protocol, one compresses the configuration from φ_g to φ , waits for time t_w before applying a shear strain $\delta\gamma$ instantaneously, and then measures the stress $\sigma_{\text{ZFC}}(\tau, t_w)$ as a function of τ . In the FC protocol, one applies $\delta\gamma$ at the initial density φ_g , and then measures the stress $\sigma_{\text{FC}}(t)$ once the configuration is compressed to φ (t is reset to zero after compression). Similar to the caging order parameters, two large-time limits can be considered: $\sigma_{\text{ZFC}} \equiv \lim_{\tau \rightarrow \infty} \lim_{t_w \rightarrow \infty} \sigma_{\text{ZFC}}(\tau, t_w)$ and $\sigma_{\text{FC}} \equiv \lim_{t_w \rightarrow \infty} \lim_{\tau \rightarrow \infty} \sigma_{\text{ZFC}}(\tau, t_w)$.

Theories have demonstrated that the above two approaches (more specifically, the caging order parameters Δ and the shear moduli $\mu = \sigma/\delta\gamma$) are intrinsically related [32]: in the large pressure limit, $\mu_{\text{ZFC}} \sim 1/\Delta_{\text{EA}}$ and $\mu_{\text{FC}}/p \sim 1/\Delta_{\text{AB}}$. These relationships are the counterpart of the duality between overlapping order parameters and magnetic susceptibilities in spin-glasses.

C. Aging effects

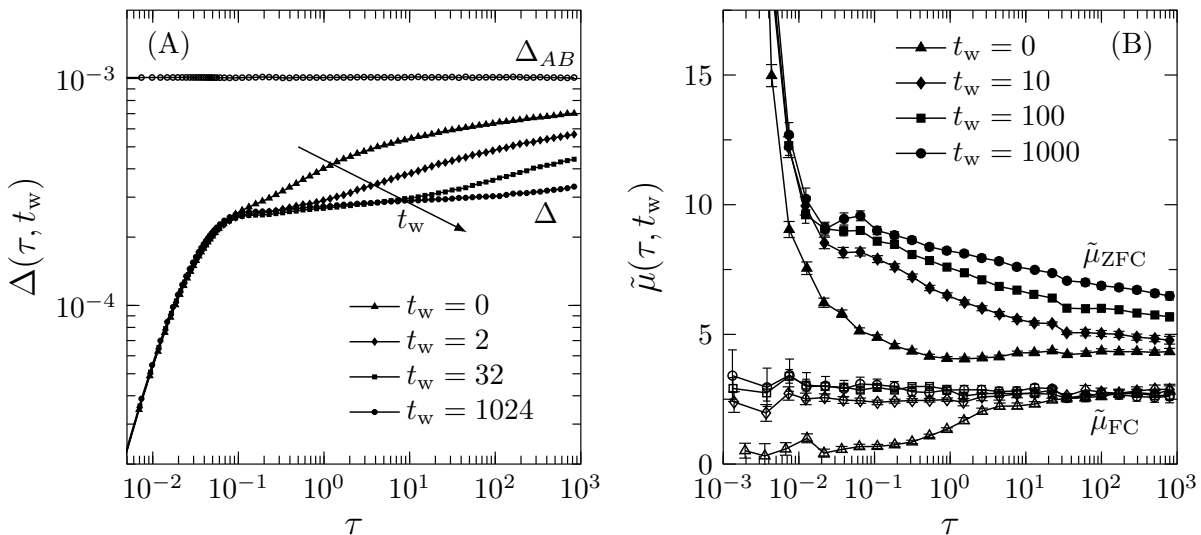


FIG. 4. Time evolutions of (A) caging order parameters (adapted from [39]) and (B) shear moduli (adapted from [47]), in the Gardner phase of the hard-sphere glass model.

In the Gardner phase ($\varphi > \varphi_G$), aging effects can be observed in both MSD (without shear deformations) and shear responses. Figure 4(A) shows the simulation data of MSD. After a short time $\tau_b \sim 1$ of ballistic motions, the evolution of $\Delta(\tau, t_w)$, as a function of τ , exhibits a plateau followed by further growth. The switch from the former to the latter happens at longer times with increasing waiting time t_w . The height of the short-time plateau gives Δ_{EA} (practically, we set $\Delta_{\text{EA}} = \Delta(\tau = \tau_b, t_w = 0)$). Figure 4(A) also displays $\Delta_{\text{AB}}(t)$, which is time-independent and should correspond to a long-time plateau of $\Delta(\tau, t_w)$ (this plateau is unfortunately beyond the current simulation time window). The clear separation of the two parameters ($\Delta_{\text{AB}} > \Delta_{\text{EA}}$) is the first numerical evidence of the ergodicity breaking in the Gardner phase [39, 48, 49].

Figure 4(B) shows the time-dependent (unitless) shear moduli, $\tilde{\mu}(\tau, t_w)$, whose behavior is similar to that of MSD. An important feature is that $\tilde{\mu}_{\text{ZFC}}(\tau, t_w)$ exhibits a plateau suggesting the existence of $\tilde{\mu}_{\text{ZFC}}$. On the other hand, $\tilde{\mu}_{\text{FC}}(t)$ is essentially a constant in time t (for $t > \tau_b$), which shall be denoted as $\tilde{\mu}_{\text{FC}}$. In the proper order of large-time limits, one expects that $\tilde{\mu}_{\text{ZFC}}(\tau, t_w)$ decays to $\tilde{\mu}_{\text{FC}}$, as $\lim_{t_w \rightarrow \infty} \lim_{\tau \rightarrow \infty} \tilde{\mu}_{\text{ZFC}}(\tau, t_w) = \tilde{\mu}_{\text{FC}}$, but the convergence becomes slower as t_w increases. Apparently $\tilde{\mu}_{\text{ZFC}}$ is larger than $\tilde{\mu}_{\text{FC}}$, which parallels $\Delta_{\text{AB}} > \Delta_{\text{EA}}$.

D. Anomalous order parameters and responses

Figure 5 shows the pressure dependence of caging order parameters (Δ_{EA} and Δ_{AB}) and shear moduli ($\tilde{\mu}_{\text{ZFC}}$ and $\tilde{\mu}_{\text{FC}}$) obtained through the above-mentioned dynamic measurements. One finds that, in the stable glass phase ($p < p_G$), $\Delta_{\text{EA}} = \Delta_{\text{AB}}$ and $\tilde{\mu}_{\text{ZFC}} = \tilde{\mu}_{\text{FC}}$, while in the Gardner phase ($p > p_G$), $\Delta_{\text{EA}} < \Delta_{\text{AB}}$ and $\tilde{\mu}_{\text{ZFC}} > \tilde{\mu}_{\text{FC}}$. In the

large pressure limit, mean-field theories predict that $\Delta_{\text{EA}} \sim p^{-\kappa}$ [50] and $\mu_{\text{ZFC}} \sim p^{\kappa}$ [32], where $\kappa = 1.41574$. The former is verified by three-dimensional simulations in Ref. [50] and the latter by those in Ref. [47] (see Fig. 5(B)). The theories also give large- p predictions $\mu_{\text{FC}}/p \sim 1/\Delta_{\text{AB}} \sim \text{constant}$, which are consistent with the simulation results in Fig. 5.

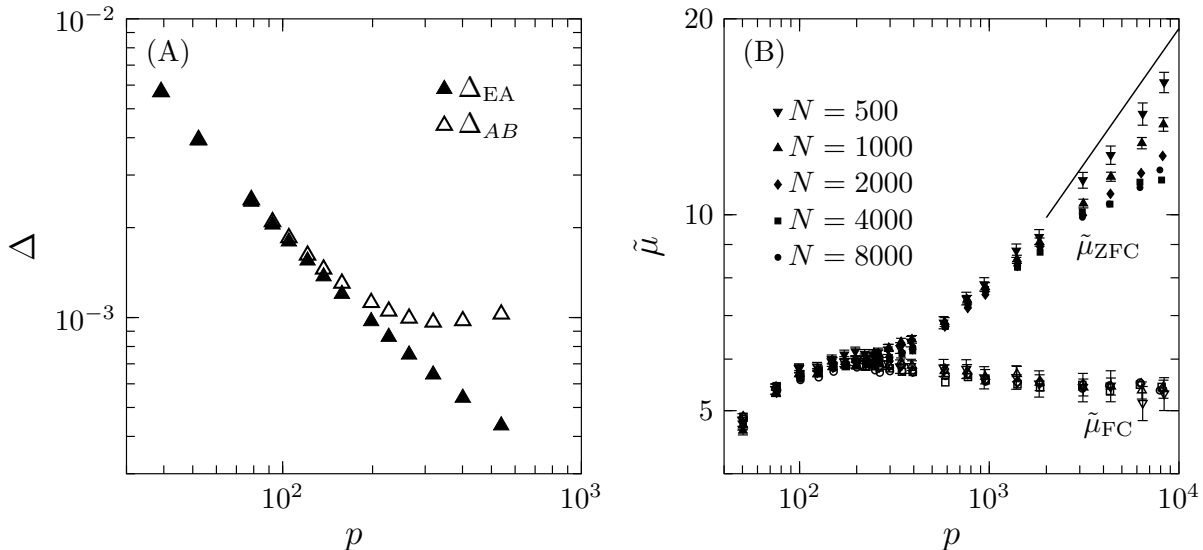


FIG. 5. (A) Bifurcation of caging order parameters Δ_{EA} and Δ_{AB} around the Gardner transition $p_{\text{G}} \approx 2.7 \times 10^2$ (adapted from [39]). (B) Protocol-dependent shear moduli $\tilde{\mu}_{\text{ZFC}}$ and $\tilde{\mu}_{\text{FC}}$ (adapted from [47]). The solid line indicates the scaling $\mu_{\text{ZFC}} \sim p^{1.41574}$ predicted by the mean-field theory [32].

III. GARDNER TRANSITION UNDER SHEAR

As predicted theoretically [51], a Gardner transition at γ_{G} could occur under shear, before the glass yields at γ_{Y} . Figure 6(A) shows the *stability map* of hard sphere glasses under shear and compression/decompression [52, 53]. The Gardner transition and yielding give rise to three types of behavior in a typical cyclic shear test (see Fig. 6(B)). (i) The stress-strain curve is reversible in the stable glass phase ($\gamma < \gamma_{\text{G}}$). (ii) If the shear strain is reversed at a maximum strain γ_{max} between γ_{G} and γ_{Y} , a hysteresis loop emerges, which however disappears below γ_{G} . This partial-reversible phenomenon is a manifestation of the hierarchical free-energy landscape consisting of basins within a common meta-basin. The part of the stress-strain curve in the Gardner phase ($\gamma_{\text{G}} < \gamma < \gamma_{\text{Y}}$) is jerky due to many small avalanches, reflecting the marginal stability. (iii) If $\gamma_{\text{max}} > \gamma_{\text{Y}}$, the cycle becomes strongly irreversible, suggesting the destruction of glass meta-basin after yielding.

IV. DISCUSSION AND OUTLOOK

As a second-order phase transition, the fluctuation of order parameters (or the susceptibility) is expected to diverge at the Gardner transition in the thermodynamic limit. Simulations have shown that the caging susceptibility grows orders of magnitude approaching the Gardner transition [39]. Furthermore, the spatial correlations between local caging order parameters become long-ranged in the Gardner phase, implying the heterogeneity of vibrational dynamics [39, 54]. However, dynamical activations could possibly turn a mean-field thermodynamic phase transition into a crossover in low dimensions. It remains inconclusive whether a sharp Gardner transition survives in three dimensions, although a renormalization group theory based on loop expansions [55] (see Chapter 3 for details) and a machine-learning facilitated finite-size analysis of simulation data [56] seem to suggest so.

The discussion so far has focused on the hard-sphere model. Hard spheres have a well-defined singularity under compression, the jamming transition, where quantities such as pressure and the length scale of mechanical response diverge (see Chapter 19 for a review on the jamming transition). Because the jamming transition lies in the Gardner phase, the full RSB predictions should also apply to the criticality and marginality of jamming, which are quantified by power-law scalings of weak forces, small interparticle gaps [50] and low-frequency vibrational modes [57]. Remarkably,

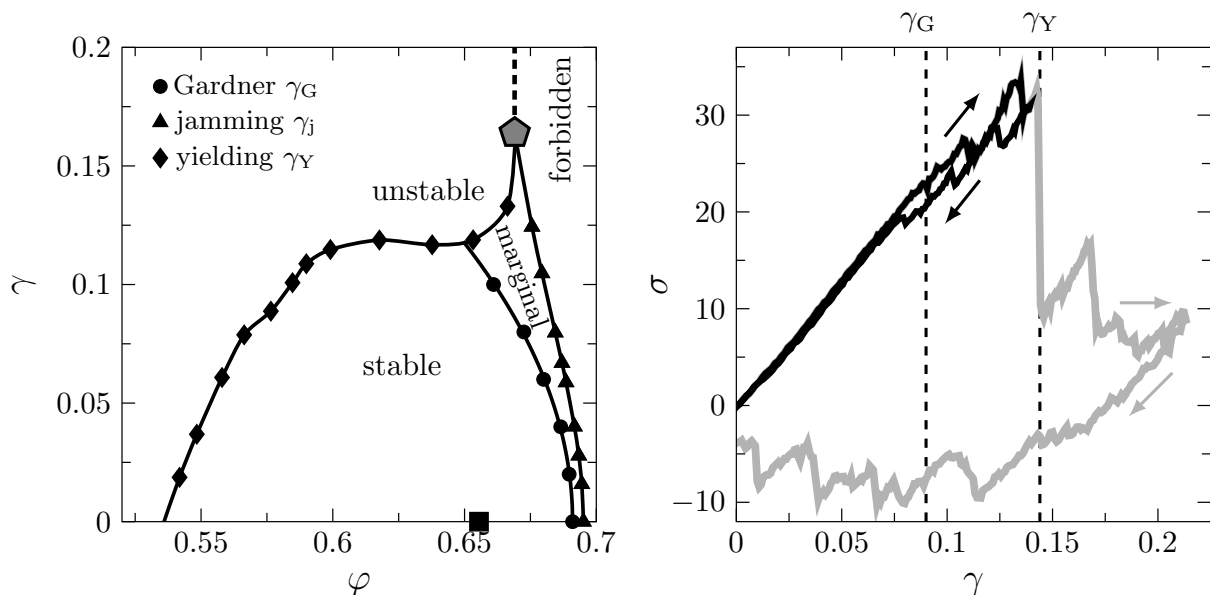


FIG. 6. (A) Stability map of hard-sphere glasses, obtained from the initial glass at $\varphi = \varphi_g$ and $\gamma = 0$ (square). (B) Stress-strain curves measured in cyclic shear simulations at a constant $\varphi = 0.66$. Black and gray lines correspond to $\gamma_G < \gamma_{\max} < \gamma_Y$ and $\gamma_{\max} > \gamma_Y$. Adapted from [52]).

numerical results seemingly agree with the mean-field exponents even in low dimensions [50, 58, 59]. The evidence of ultrametricity that characterizes the hierarchical energy landscape, has also been demonstrated numerically in jammed packings in three dimensions [60].

The Gardner transition seems to emerge as a “precursor” of certain singularities (jamming under compression and yielding under shear) in hard particles. The situation is more complicated in cases without such singularities, e.g., cooling soft spheres under the constant density condition. On the one hand, the mean-field theory universally identifies the existence of Gardner transition in soft spheres [61], and simulations have reported a rejuvenation-memory effect [62] similar to that found in spin-glasses. On the other hand, however, simulations demonstrate that the Gardner transition could be interfered with by low-dimensional effects such as localized “defects” [63]. Separating the Gardner physics from strong low-dimensional effects in soft spheres remains a challenge in simulations.

Finally, experimental efforts to detect the Gardner transition have shown encouraging progress. The caging order parameter approach is applied to vibrated granular discs, providing evidence of the Gardner phase [64]. In the Gardner phase, one expects a logarithmic growth of the MSD with lag time, which is verified in an experiment of glassy colloidal suspensions [65]. The experimental data of shear modulus and MSD in a hard-sphere colloidal glass are consistent with the scalings $\mu_{ZFC} \sim 1/\Delta_{EA} \sim p^\kappa$ [66]. The critical scalings of weak forces and small interparticle gaps have also been verified by precise experimental measurements of jammed photo-elastic disks [67]. The evidence of a Gardner-like transition is reported in a two-dimensional bidisperse granular crystal [68], suggesting that the Gardner physics could be observed with minimum disorder [69]. Examining protocol-dependent shear moduli and complex aging dynamics could provide future directions for the experimental exploration of Gardner physics.

-
- [1] Giorgio Parisi, Pierfrancesco Urbani, and Francesco Zamponi, *Theory of Simple Glasses: Exact Solutions in Infinite Dimensions* (Cambridge University Press, 2020).
 - [2] Ludovic Berthier, Giulio Biroli, Patrick Charbonneau, Eric I Corwin, Silvio Franz, and Francesco Zamponi, “Gardner physics in amorphous solids and beyond,” *The Journal of chemical physics* **151**, 010901 (2019).
 - [3] M. Mézard, G. Parisi, and M. A. Virasoro, *Spin glass theory and beyond* (World Scientific, Singapore, 1987).
 - [4] Shoichi Nagata, PH Keesom, and HR Harrison, “Low-dc-field susceptibility of cu mn spin glass,” *Physical Review B* **19**, 1633 (1979).
 - [5] Samuel Frederick Edwards and Phil W Anderson, “Theory of spin glasses,” *Journal of Physics F: Metal Physics* **5**, 965 (1975).
 - [6] Tommaso Castellani and Andrea Cavagna, “Spin-glass theory for pedestrians,” *Journal of Statistical Mechanics: Theory and Experiment* **2005**, P05012 (2005).

- [7] P Granberg, L Sandlund, P Nordblad, P Svedlindh, and L Lundgren, “Observation of a time-dependent spatial correlation length in a metallic spin glass,” *Physical Review B* **38**, 7097 (1988).
- [8] Eric Vincent, Jacques Hammann, Miguel Ocio, Jean-Philippe Bouchaud, and Leticia F Cugliandolo, “Slow dynamics and aging in spin glasses,” in *Complex Behaviour of Glassy Systems* (Springer, 1997) pp. 184–219.
- [9] Per Nordblad and Peter Svedlindh, “Experiments on spin glasses,” in *Spin Glasses and Random Fields* (World Scientific, 1998) pp. 1–27.
- [10] Leticia F Cugliandolo and Jorge Kurchan, “Analytical solution of the off-equilibrium dynamics of a long-range spin-glass model,” *Physical Review Letters* **71**, 173 (1993).
- [11] Leticia F Cugliandolo and Jorge Kurchan, “On the out-of-equilibrium relaxation of the sherrington-kirkpatrick model,” *Journal of Physics A: Mathematical and General* **27**, 5749 (1994).
- [12] Leticia F Cugliandolo, Jorge Kurchan, and Luca Peliti, “Energy flow, partial equilibration, and effective temperatures in systems with slow dynamics,” *Physical Review E* **55**, 3898 (1997).
- [13] Silvio Franz, Marc Mézard, Giorgio Parisi, and Luca Peliti, “Measuring equilibrium properties in aging systems,” *Physical Review Letters* **81**, 1758 (1998).
- [14] Enzo Marinari, Giorgio Parisi, Federico Ricci-Tersenghi, and Juan J Ruiz-Lorenzo, “Off-equilibrium dynamics at very low temperatures in three-dimensional spin glasses,” *Journal of Physics A: Mathematical and General* **33**, 2373 (2000).
- [15] Hajime Yoshino, Koji Hukushima, and Hajime Takayama, “Extended droplet theory for aging in short-range spin glasses and a numerical examination,” *Physical Review B* **66**, 064431 (2002).
- [16] Alan J Bray and Michael A Moore, “Chaotic nature of the spin-glass phase,” *Physical review letters* **58**, 57 (1987).
- [17] Daniel S Fisher and David A Huse, “Equilibrium behavior of the spin-glass ordered phase,” *Physical Review B* **38**, 386 (1988).
- [18] Daniel S Fisher and David A Huse, “Nonequilibrium dynamics of spin glasses,” *Physical Review B* **38**, 373 (1988).
- [19] I Kondor, “On chaos in spin glasses,” *Journal of Physics A: Mathematical and General* **22**, L163 (1989).
- [20] Tommaso Rizzo and Andrea Crisanti, “Chaos in temperature in the sherrington-kirkpatrick model,” *Physical review letters* **90**, 137201 (2003).
- [21] Tommaso Rizzo and Hajime Yoshino, “Chaos in glassy systems from a thouless-anderson-palmer perspective,” *Physical Review B* **73**, 064416 (2006).
- [22] Hajime Yoshino and Tommaso Rizzo, “Stepwise responses in mesoscopic glassy systems: A mean-field approach,” *Physical Review B* **77**, 104429 (2008).
- [23] Giorgio Parisi and Tommaso Rizzo, “Chaos in temperature in diluted mean-field spin-glass,” *Journal of Physics A: Mathematical and Theoretical* **43**, 235003 (2010).
- [24] Pierre Le Doussal, Markus Müller, and Kay Jörg Wiese, “Avalanches in mean-field models and the barkhausen noise in spin-glasses,” *EPL (Europhysics Letters)* **91**, 57004 (2010).
- [25] Pierre Le Doussal, Markus Müller, and Kay Jörg Wiese, “Equilibrium avalanches in spin glasses,” *Physical Review B* **85**, 214402 (2012).
- [26] Silvio Franz and Stefano Spigler, “Mean-field avalanches in jammed spheres,” *Physical Review E* **95**, 022139 (2017).
- [27] K Jonason, E Vincent, J Hammann, JP Bouchaud, and P Nordblad, “Memory and chaos effects in spin glasses,” *Physical Review Letters* **81**, 3243 (1998).
- [28] Hajime Yoshino, Anaël Lemaitre, and J-P Bouchaud, “Multiple domain growth and memory in the droplet model for spin-glasses,” *The European Physical Journal B-Condensed Matter and Complex Systems* **20**, 367–395 (2001).
- [29] PE Jönsson, R Mathieu, Per Nordblad, H Yoshino, H Aruga Katori, and A Ito, “Nonequilibrium dynamics of spin glasses: Examination of the ghost domain scenario,” *Physical Review B* **70**, 174402 (2004).
- [30] Hajime Yoshino and Marc Mézard, “Emergence of rigidity at the structural glass transition: A first-principles computation,” *Physical review letters* **105**, 015504 (2010).
- [31] Hajime Yoshino, “Replica theory of the rigidity of structural glasses,” *The Journal of Chemical Physics* **136**, 214108 (2012).
- [32] Hajime Yoshino and Francesco Zamponi, “Shear modulus of glasses: Results from the full replica-symmetry-breaking solution,” *Physical Review E* **90**, 022302 (2014).
- [33] Thibaud Maimbourg, Jorge Kurchan, and Francesco Zamponi, “Solution of the dynamics of liquids in the large-dimensional limit,” *Physical review letters* **116**, 015902 (2016).
- [34] Jorge Kurchan, Thibaud Maimbourg, and Francesco Zamponi, “Statics and dynamics of infinite-dimensional liquids and glasses: a parallel and compact derivation,” *Journal of Statistical Mechanics: Theory and Experiment* **2016**, 033210 (2016).
- [35] Elisabeth Agoritsas, Thibaud Maimbourg, and Francesco Zamponi, “Out-of-equilibrium dynamical equations of infinite-dimensional particle systems i. the isotropic case,” *Journal of Physics A: Mathematical and Theoretical* **52**, 144002 (2019).
- [36] Elisabeth Agoritsas, Thibaud Maimbourg, and Francesco Zamponi, “Out-of-equilibrium dynamical equations of infinite-dimensional particle systems. ii. the anisotropic case under shear strain,” *Journal of Physics A: Mathematical and Theoretical* **52**, 334001 (2019).
- [37] WGT Kranendonk and D Frenkel, “Computer simulation of solid-liquid coexistence in binary hard sphere mixtures,” *Molecular physics* **72**, 679–697 (1991).
- [38] Tomás S Grigera and Giorgio Parisi, “Fast monte carlo algorithm for supercooled soft spheres,” *Physical Review E* **63**, 045102 (2001).
- [39] Ludovic Berthier, Patrick Charbonneau, Yuliang Jin, Giorgio Parisi, Beatriz Seoane, and Francesco Zamponi, “Growing timescales and lengthscales characterizing vibrations of amorphous solids,” *Proceedings of the National Academy of Sciences* **113**, 8397–8401 (2016).
- [40] Boris D Lubachevsky and Frank H Stillinger, “Geometric properties of random disk packings,” *Journal of statistical Physics*

- 60**, 561–583 (1990).
- [41] Martin Goldstein, “Communications: Comparison of activation barriers for the Johari–Goldstein and alpha relaxations and its implications,” *J. Chem. Phys.* **132**, 041104 (2010).
 - [42] T. Boublik, “Hard sphere equation of state,” *J. Chem. Phys.* **53**, 471 (1970).
 - [43] Patrick Charbonneau, Yuliang Jin, Giorgio Parisi, and Francesco Zamponi, “Hopping and the Stokes–Einstein relation breakdown in simple glass formers,” *Proc. Natl. Acad. Sci. U.S.A.* **111**, 15025–15030 (2014).
 - [44] Aleksandar Donev, Salvatore Torquato, and Frank H Stillinger, “Pair correlation function characteristics of nearly jammed disordered and ordered hard-sphere packings,” *Physical Review E* **71**, 011105 (2005).
 - [45] Jean-Philippe Bouchaud, Leticia F Cugliandolo, Jorge Kurchan, and Marc Mézard, “Out of equilibrium dynamics in spin-glasses and other glassy systems,” *Spin glasses and random fields* **12**, 161 (1998).
 - [46] AW Lees and SF Edwards, “The computer study of transport processes under extreme conditions,” *J. Phys. Condens. Matter* **5**, 1921 (1972).
 - [47] Yuliang Jin and Hajime Yoshino, “Exploring the complex free-energy landscape of the simplest glass by rheology,” *Nature communications* **8**, 1–8 (2017).
 - [48] Patrick Charbonneau, Yuliang Jin, Giorgio Parisi, Corrado Rainone, Beatriz Seoane, and Francesco Zamponi, “Numerical detection of the gardner transition in a mean-field glass former,” *Physical Review E* **92**, 012316 (2015).
 - [49] Beatriz Seoane and Francesco Zamponi, “Spin-glass-like aging in colloidal and granular glasses,” *Soft Matter* **14**, 5222–5234 (2018).
 - [50] Patrick Charbonneau, Jorge Kurchan, Giorgio Parisi, Pierfrancesco Urbani, and Francesco Zamponi, “Fractal free energy landscapes in structural glasses,” *Nature communications* **5**, 1–6 (2014).
 - [51] Corrado Rainone, Pierfrancesco Urbani, Hajime Yoshino, and Francesco Zamponi, “Following the evolution of hard sphere glasses in infinite dimensions under external perturbations: Compression and shear strain,” *Physical review letters* **114**, 015701 (2015).
 - [52] Yuliang Jin, Pierfrancesco Urbani, Francesco Zamponi, and Hajime Yoshino, “A stability-reversibility map unifies elasticity, plasticity, yielding, and jamming in hard sphere glasses,” *Science advances* **4**, eaat6387 (2018).
 - [53] Ada Altieri and Francesco Zamponi, “Mean-field stability map of hard-sphere glasses,” *Physical Review E* **100**, 032140 (2019).
 - [54] Qinyi Liao and Ludovic Berthier, “Hierarchical landscape of hard disk glasses,” *Physical Review X* **9**, 011049 (2019).
 - [55] Patrick Charbonneau and Sho Yaida, “Nontrivial critical fixed point for replica-symmetry-breaking transitions,” *Physical review letters* **118**, 215701 (2017).
 - [56] Huaping Li, Yuliang Jin, Ying Jiang, and Jeff ZY Chen, “Determining the nonequilibrium criticality of a gardner transition via a hybrid study of molecular simulations and machine learning,” *Proceedings of the National Academy of Sciences* **118** (2021).
 - [57] Silvio Franz, Giorgio Parisi, Pierfrancesco Urbani, and Francesco Zamponi, “Universal spectrum of normal modes in low-temperature glasses,” *Proceedings of the National Academy of Sciences* **112**, 14539–14544 (2015).
 - [58] Patrick Charbonneau, Eric I Corwin, Giorgio Parisi, and Francesco Zamponi, “Jamming criticality revealed by removing localized buckling excitations,” *Physical review letters* **114**, 125504 (2015).
 - [59] Patrick Charbonneau, Eric I Corwin, Giorgio Parisi, Alexis Poncet, and Francesco Zamponi, “Universal non-debye scaling in the density of states of amorphous solids,” *Physical review letters* **117**, 045503 (2016).
 - [60] RC Dennis and EI Corwin, “Jamming energy landscape is hierarchical and ultrametric,” *Physical review letters* **124**, 078002 (2020).
 - [61] Camille Scalliet, Ludovic Berthier, and Francesco Zamponi, “Marginally stable phases in mean-field structural glasses,” *Physical Review E* **99**, 012107 (2019).
 - [62] Camille Scalliet and Ludovic Berthier, “Rejuvenation and memory effects in a structural glass,” *Physical review letters* **122**, 255502 (2019).
 - [63] Camille Scalliet, Ludovic Berthier, and Francesco Zamponi, “Absence of marginal stability in a structural glass,” *Physical review letters* **119**, 205501 (2017).
 - [64] Antoine Seguin and Olivier Dauchot, “Experimental evidence of the gardner phase in a granular glass,” *Physical review letters* **117**, 228001 (2016).
 - [65] Andrew P Hammond and Eric I Corwin, “Experimental observation of the marginal glass phase in a colloidal glass,” *Proceedings of the National Academy of Sciences* **117**, 5714–5718 (2020).
 - [66] Rojman Zargar, Eric DeGiuli, and Daniel Bonn, “Scaling for hard-sphere colloidal glasses near jamming,” *EPL (Europhysics Letters)* **116**, 68004 (2017).
 - [67] Yinqiao Wang, Jin Shang, Yuliang Jin, and Jie Zhang, “Experimental observations of marginal criticality in granular materials,” *Proceedings of the National Academy of Sciences* **119**, e2204879119 (2022).
 - [68] Lars Kool, Patrick Charbonneau, and Karen E Daniels, “Gardner-like transition from variable to persistent force contacts in granular crystals,” *arXiv preprint arXiv:2205.06794* (2022).
 - [69] Patrick Charbonneau, Eric I Corwin, Lin Fu, Georgios Tsekenis, and Michael van Der Naald, “Glassy, gardner-like phenomenology in minimally polydisperse crystalline systems,” *Physical Review E* **99**, 020901 (2019).